

# FlashOptim: Optimizers for Memory Efficient Training

Jose Javier Gonzalez Ortiz\*  
Databricks AI Research  
j.gonzalez@databricks.com

Abhay Gupta  
Databricks AI Research  
abhay.gupta@databricks.com

Chris Renard  
Databricks AI Research<sup>†</sup>  
chris@standardkernel.co

Davis Blalock\*  
Databricks AI Research<sup>‡</sup>  
daviswblalock@gmail.com

## Abstract

Standard mixed-precision training of neural networks requires many bytes of accelerator memory for each model parameter. These bytes reflect not just the parameter itself, but also its gradient and one or more optimizer state variables. With each of these values typically requiring 4 bytes, training even a 7 billion parameter model can be impractical for researchers with less than 100GB of accelerator memory.

We introduce FlashOptim, a suite of optimizations that reduces per-parameter memory by over 50% while preserving model quality and API compatibility. Our approach introduces two key techniques. First, we improve master weight splitting by finding and exploiting a tight bound on its quantization error. Second, we design companding functions that greatly reduce the error in 8-bit optimizer state quantization. Together with 16-bit gradients, these techniques reduce AdamW memory from 16 bytes to 7 bytes per parameter, or 5 bytes with gradient release. They also cut model checkpoint sizes by more than half.

Experiments with FlashOptim applied to SGD, AdamW, and Lion show no measurable quality degradation on any task from a collection of standard vision and language benchmarks, including Llama-3.1-8B finetuning.

## 1. Introduction

Recent advances in deep learning have been driven largely by scaling: larger models trained on more data consistently yield better results across language (Kaplan et al., 2020; Hoffmann et al., 2022; Chowdhery et al., 2023) and vision (Rosenfeld et al., 2019; Tan and Le, 2019; Dehghani et al., 2023) domains. Training large models can require a great deal of accelerator memory, with each training iteration

Table 1: **Memory per parameter (bytes) for model training.** FlashOptim reduces Adam from 16 to 7 bytes and SGD from 12 to 6 bytes. (★) With gradient release, we further reduce total memory requirements by 2 bytes.

Tensor	SGD	FlashSGD	Adam	FlashAdam
Master Weights	4	2	4	2
Weight Correction		1		1
Gradients	4	2 (0★)	4	2 (0★)
Momentum	4	1	4	1
Variance			4	1
<b>Total</b>	<b>12</b>	<b>6 (4★)</b>	<b>16</b>	<b>7 (5★)</b>

requiring memory to store parameters, activations, gradients, and optimizer state.

How much memory do these tensors require? Table 1 shows a typical breakdown. Excluding activations, which scale with batch size rather than parameter count, training with Adam uses about 16 bytes per parameter. Training a 7-billion-parameter LLM therefore requires at least 112GB of accelerator memory, plus more memory for activations.

Several approaches mitigate this memory consumption. Distributed training with tensor sharding (Rajbhandari et al., 2020) divides the memory load across multiple accelerators. While this is standard practice in well-resourced organizations, it requires access to multiple accelerators that many practitioners lack. Another alternative is to perform CPU offloading (Ren et al., 2021), which moves some tensors to host memory at the cost of added overhead and complexity. Third, parameter-efficient methods (Li and Liang, 2021; Hu et al., 2022) reduce trainable parameters by freezing most weights and training either a small subset of the original weights or a small set of new auxiliary weights, but fundamentally alter the training dynamics (Biderman et al., 2024).

In this work, we describe FlashOptim, a set of techniques

\*Equal contribution

<sup>†</sup>Now at Standard Kernel Co.

<sup>‡</sup>Now at Google DeepMind

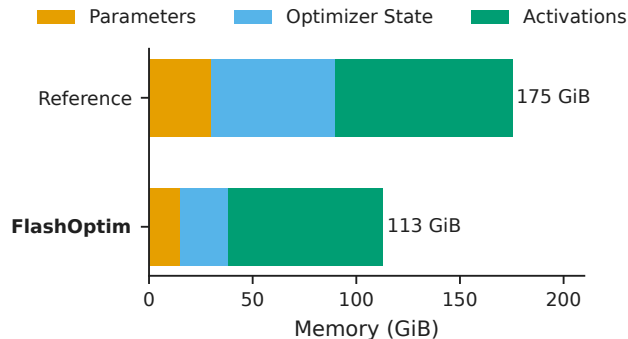


Figure 1: **Memory breakdown for finetuning Llama-3.1-8B.** FlashOptim reduces peak memory from 175 to 113 GiB by compressing parameters and optimizer states.

to reduce parameter-associated memory in common deep learning optimizers. Figure 1 shows an example: with FlashOptim, finetuning Llama-3.1-8B drops from 175 GiB to 113 GiB peak memory. Crucially, these memory savings are effectively free—FlashOptim runs just as fast as standard optimizers and causes no measurable loss of model quality across a suite of established training tasks (§4). This allows our optimizer implementations to serve as drop-in replacements for their unoptimized counterparts. FlashOptim incorporates existing enhancements, such as gradient release (Zhang et al., 2023; Warner, 2024), while also introducing improved float splitting (Zamirai et al., 2020; Warner, 2024) and simplified 8-bit optimizer state quantization (Dettmers et al., 2022; Peng et al., 2023; Xi et al., 2025; Fishman et al., 2025). Furthermore, FlashOptim composes cleanly with existing memory-reduction techniques, such as sharding tensors across accelerators, offloading to CPU, or freezing parameters.

We make the following contributions:

- **Improved float splitting:** Instead of materializing both a 32-bit master weight and a 16-bit downcast weight for forward and backward, one can split each master weight into a low-precision weight and a correction term stored in the optimizer (Zamirai et al., 2020; Warner, 2024). We improve on existing float splitting techniques by (a) enabling either 8- or 16-bit error correction and (b) achieving much lower reconstruction error for a given number of correction bits. This allows us to use 24-bit master weights with no loss of model quality.
- **Companded optimizer state quantization:** Several works have shown that one can compress optimizer states to 8 bits per element given sufficient software complexity. We demonstrate that one can do this much more simply, with nothing more than a one-line preprocessing function before standard group-wise linear quantization. Our ablations across different tensor types

suggest that designing custom companding functions is a fruitful direction for future research.

- **Fused optimized kernels:** We implement FlashOptim as optimizer step kernels that fuse all compression and quantization operations, reducing memory while preserving throughput during training. Our implementation is publicly available at <https://github.com/databricks/flashoptim>.

## 2. Related Work

**Low-Precision Training.** Mixed-precision training (Micikevicius et al., 2018) executes forward and backward passes in FP16 to reduce memory and compute, while retaining FP32 precision for optimizer states and master weights to preserve numerical stability. Kalamkar et al. (2019) showed that BFloat16 (Google, 2019) works equally well, and Zamirai et al. (2020) explored pure BF16 master weights with stochastic rounding and Kahan summation. Recent work has pushed further with FP8 training (Wang et al., 2018; Mellempudi et al., 2019; Micikevicius et al., 2022; Fishman et al., 2025; Narayan et al., 2025), though these approaches primarily target compute formats and retain higher-precision storage for master weights. FlashOptim extends this line of work with an improved float splitting mechanism that reduces storage to 3 bytes per parameter, down from 4-byte FP32, while maintaining FP32-equivalent training semantics.

**Optimizer State Compression.** Dettmers et al. (2022) applied 8-bit block-wise dynamic quantization to Adam’s momentum and variance, reducing optimizer state from 8 to 2 bytes per parameter. Follow-up work explored FP8 representations (Peng et al., 2023; Xi et al., 2025; Fishman et al., 2025), and Li et al. (2023) compressed both moments to 4-bit using row and column-wise quantization. MicroAdam (Modoranu et al., 2024) instead compresses gradients before updating optimizer states. Rather than design elaborate quantization methods or number formats, we show that one can obtain 8-bit optimizer states with no quality loss using simple, one-line preprocessing functions. Beyond optimizer states, we address additional sources of per-parameter memory, eliminating entire bytes from other tensors.

**Gradient Memory and Communication.** LOMO (Lv et al., 2024b), AdaLOMO (Lv et al., 2024a), and Adam Accumulation (Zhang et al., 2023) fuse parameter updates into the backward pass to release gradient memory eagerly. However, this conflicts with gradient accumulation, which requires the full accumulated gradient before updating. In distributed settings, gradient communication can also become a bottleneck. One can reduce this bottleneck by, e.g., compressing gradients to 1-bit with error feedback (Tang et al., 2021), or using low-rank approximations (Vogels et al., 2019). FlashOptim supports gradient release when compatible and could be used alongside communication compression

techniques.

**Memory-Efficient Optimization.** Alternative optimizer designs reduce memory by restructuring update rules and stored buffers. Adafactor (Shazeer and Stern, 2018) achieves sublinear memory by factorizing the second moment into row and column statistics; SM3 (Anil et al., 2019) stores structured maxima; NovoGrad (Ginsburg et al., 2019) replaces per-parameter variance with layer-wise normalization. Adam-mini (Zhang et al., 2025) shares variance terms across parameter blocks, while Adapprox (Zhao et al., 2024b) uses a low-rank approximation. Other approaches eliminate the second moment entirely: Lion (Chen et al., 2023) uses sign-based momentum, and Muon (Jordan et al., 2024; Liu et al., 2025) applies orthogonalized updates. Pethick et al. (2025) extend Muon to unify gradient accumulation with momentum, removing dedicated optimizer memory altogether.

Low-rank decompositions approximate full tensors while requiring less memory. For fine-tuning, LoRA (Hu et al., 2022) and QLoRA (Detmers et al., 2023) freeze base weights and train only low-rank adapters. For pretraining, GaLore (Zhao et al., 2024a) projects gradients to a low-rank subspace, and APOLLO (Zhu et al., 2025) approximates adaptive scaling with random projections. Unlike these approaches that modify the optimizer’s update rule, FlashOptim preserves standard optimizer semantics and can be combined with these techniques.

**System-Level Memory Optimizations.** System-level approaches reduce accelerator memory without changing optimization semantics. Activation checkpointing (Chen et al., 2016; Korthikanti et al., 2023) trades compute for memory by recomputing activations during the backward pass. ZeRO (Rajbhandari et al., 2020) partitions optimizer states, gradients, and parameters across data-parallel ranks, while offloading (Rajbhandari et al., 2021; Ren et al., 2021) moves state to CPU or NVMe memory. FlashOptim is orthogonal to these approaches: it reduces the per-rank footprint and can be used with ZeRO, FSDP (Zhao et al., 2023), and activation checkpointing.

### 3. Method

This section describes the two key techniques behind FlashOptim: weight splitting (§3.1) and companded optimizer state quantization (§3.2). We then describe how to integrate these ideas into common optimizer updates while minimizing associated overhead (§3.3).

#### 3.1. Weight Splitting

Mixed-precision training uses 16-bit weights for forward and backward passes, but accumulating gradient updates requires higher precision to avoid stagnation (Micikevicius et al., 2018). Thus, the standard practice is to maintain FP32 precision master weights during training.

However, this introduces waste: the downcast weights take space, but store no information beyond what’s saved in the master weights. To eliminate this redundancy, weight splitting (Zamirai et al., 2020; Warner, 2024) instead stores the downcast weights and narrow error-correction values. By combining a 16-bit weight  $\theta'$  with a 16-bit error correction value  $\rho$ , one has enough information to reconstruct a 32-bit master weight  $\theta$  with no redundancy.

The core questions in a weight splitting scheme are 1) how to set  $(\theta', \rho)$  given  $\theta$  and 2) how to estimate  $\theta$  given  $(\theta', \rho)$ . One obvious approach is to use the high 16 bits of  $\theta$  as  $\theta'$  and the low 16 bits as  $\rho$ . This admits exact reconstruction of  $\theta$  for the special case of BF16  $\theta'$  and FP32  $\theta$ , since these formats happen to share the same exponent sizes and offsets. However, this approach doesn’t generalize to other pairs of number formats. It also rounds towards zero instead of towards the nearest low-precision value.

A more general alternative, used in previous work (Zamirai et al., 2020; Warner, 2024), is to set  $\rho = \theta - \theta'$ , represented as a BF16 value. The problem with this is that the difference of two floating-point numbers requires as many bits to store exactly as the wider of the two floats.<sup>1</sup> This means that a BF16  $\rho$  incurs approximation error. E.g., if the rounding error were  $1e-5$ , BF16 could only represent  $1.0014e-5$ . In general, while BF16’s wide exponent lets it represent nearly the full range of FP32, its 7 mantissa bits only guarantee a relative error bound of  $1/256$ .

Our observation is that **all exponent bits in this scheme are wasted**. The exponent of  $e \triangleq \theta - \theta'$  can always be inferred from  $\theta'$ : under round-to-nearest,  $\theta$  must lie within  $[\theta' - u/2, \theta' + u/2]$ , where  $u = \text{ULP}(\theta')$  is the unit in the last place (Goldberg, 1991). If  $\theta$  were outside this interval, it would have rounded to a different value. It therefore suffices to encode where  $e$  falls within this tiny interval rather than across the full FP32 range.

To exploit this observation, we rescale  $e$  such that  $[-u/2, u/2]$  maps to  $[-N, N]$ ;  $N \triangleq 2^b - 1$  and then quantize this rescaled  $e$  to the nearest  $b$ -bit integer. That is,

$$\begin{aligned} \theta' &= \text{downcast}(\theta) \\ \rho &= \text{round} \left( \frac{\theta - \theta'}{\text{ULP}(\theta')/2} \cdot N \right), \end{aligned} \tag{1}$$

To reconstruct  $\theta$  from  $(\theta', \rho)$ , we invert this scaling and add the result to  $\theta'$ .

$$\hat{\theta} = \theta' + \frac{\rho}{N} \cdot \frac{\text{ULP}(\theta')}{2} \tag{2}$$

For tensors of floating-point values we apply this transformation elementwise. Algorithm 1 provides a lower-level description of the compression and decompression operations with numerical precision considerations.

<sup>1</sup>Consider, e.g., storing the minimum float32 subnormal, which will be rounded to zero by any narrower datatype.

---

**Algorithm 1** Weight Splitting

---

**Constants:**  $N$  (127 for INT8, 32767 for int16)

```
1: function  $\mathcal{C}(\theta)$ 
2:    $\theta' \leftarrow \text{Downcast}(\theta)$ 
3:    $e \leftarrow \theta - \text{Float32}(\theta')$ 
4:    $\ell \leftarrow \lfloor \log_2 \text{ULP}(\theta') \rfloor - 1$ 
5:    $h \leftarrow \lfloor -\ell/2 \rfloor$  // For numerical stability
6:    $e_{\text{norm}} \leftarrow (e \cdot 2^h) \cdot 2^{-\ell-h}$ 
7:    $\rho \leftarrow \text{Int}(\text{Round}(\text{Clamp}(e_{\text{norm}}, -1, 1) \cdot N))$ 
8:   return  $\theta', \rho$ 
9: function  $\mathcal{C}^{-1}(\theta', \rho)$ 
10:   $\ell \leftarrow \lfloor \log_2 \text{ULP}(\theta') \rfloor - 1$ 
11:   $h \leftarrow \lfloor \ell/2 \rfloor$ 
12:   $e \leftarrow ((\text{Float32}(\rho)/N) \cdot 2^h) \cdot 2^{\ell-h}$ 
13:  return  $\text{Float32}(\theta') + e$ 
```

---

When using BF16 for  $\theta'$  and INT8 for  $\rho$ , the compressed representation provides approximately 24 bits of effective precision (16 from BF16 plus 8 from the error term). This is analogous to the PXR24 format used in high-dynamic-range imaging, which achieves similar precision by rounding 32-bit floats to 24 bits (Kainz et al., 2004).

### 3.2. Companded Optimizer State Quantization

For optimizer state variables such as momentum and variance estimates, a common approach is group-wise quantization: dividing tensors into fixed-length groups and mapping values to a lower-precision format like INT8 (Dettmers et al., 2022). To increase the precision range of the group of values, they are rescaled using the maximum absolute value (*absmax*), which is stored as an additional scale with 32 or 16 bits of precision. While simple, this *uniform* quantization allocates bins evenly across the value range, implicitly assuming that values are roughly uniformly distributed. Our measurements show that optimizer state distributions violate this assumption, and we find that applying nonlinear *companding* functions before quantization can reshape these distributions toward uniformity, improving utilization of quantization bins and reducing quantization error. As we show in §4.5, this companding step is critical: without it, linear quantization of optimizer states causes training to diverge.

We design specialized transformations for each optimizer state type. For momentum tensors (used in SGD, Adam, and Lion), we first normalize each group by its *absmax* scale, then apply a softsign-like function:

$$\phi_m(x) = \frac{2x}{1 + |x|} \quad \phi_m^{-1}(z) = \frac{z}{2 - |z|} \quad (3)$$

This function compresses extreme values: inputs near  $\pm 1$  are pushed toward the center, spreading the momentum distribution more evenly across quantization bins. In contrast,

---

**Algorithm 2**  $\mathcal{Q}_m$ : Momentum Quantization

---

**Constants:** Group size  $G = 32$

```
1: function  $\mathcal{Q}_m(m)$ 
2:   for each group  $g$  of  $G$  elements do
3:      $s_g \leftarrow \max(|m_g|)$ 
4:      $m'_g \leftarrow m_g/s_g$ 
5:      $m''_g \leftarrow 2m'_g/(1 + |m'_g|)$ 
6:      $m^q_g \leftarrow \text{Round}(m''_g \cdot 127, \text{INT8})$ 
7:   return  $m^q, s$ 
8: function  $\mathcal{Q}_m^{-1}(m^q, s)$ 
9:   for each group  $g$  do
10:     $m''_g \leftarrow m^q_g/127$ 
11:     $m'_g \leftarrow m''_g/(2 - |m''_g|)$ 
12:     $m_g \leftarrow m'_g \cdot s_g$ 
13:  return  $m$ 
```

---

---

**Algorithm 3**  $\mathcal{Q}_v$ : Variance Quantization

---

**Constants:** Group size  $G = 32$

```
1: function  $\mathcal{Q}_v(v)$ 
2:    $v' \leftarrow \sqrt{v}$ 
3:   for each group  $g$  of  $G$  elements do
4:      $s_g \leftarrow \max(v'_g)$ 
5:      $v^q_g \leftarrow \text{Round}((v'_g/s_g) \cdot 255, \text{UINT8})$ 
6:   return  $v^q, s$ 
7: function  $\mathcal{Q}_v^{-1}(v^q, s)$ 
8:   for each group  $g$  do
9:      $v'_g \leftarrow (v^q_g/255) \cdot s_g$ 
10:     $v_g \leftarrow (v'_g)^2$ 
11:  return  $v$ 
```

---

for variance tensors in Adam, we first apply a square root, then normalize by the group *absmax*:

$$\phi_v(x) = \sqrt{x} \quad \phi_v^{-1}(z) = z^2 \quad (4)$$

Here the square root is motivated by Adam’s variance update  $v_t = \beta_2 v_{t-1} + (1 - \beta_2) g^2$  that accumulates squared gradients, producing heavy-tailed distributions with large dynamic range. Both transformations satisfy key design criteria: they are exactly invertible, computationally efficient (one division or square root per element), their inverses are computationally efficient, and require no hyperparameters.

For both momentum and variance, we partition the tensor into groups of  $G = 32$  elements and store a separate FP16 scale factor per group, introducing an overhead of  $2/G = 1/16$  bytes per parameter. We store the normalized momentum in signed integers (INT8) and variance in unsigned integers (UINT8) since it is non-negative. Algorithms 2 and 3 detail the quantization and dequantization procedures for momentum and variance respectively.

**Algorithm 4** FlashAdamW: Memory-Efficient AdamW. We highlight the changes from AdamW.

**Require:** Parameters  $\theta_0$ , learning rate schedule  $\{\eta_t\}_{t=1}^T$ ,  $\beta_1, \beta_2 \in [0, 1)$ ,  $\varepsilon > 0$ , weight decay  $\lambda \geq 0$ , loss  $\mathcal{L}(\theta)$ , minibatch sampler  $\mathcal{B}(\cdot)$

- 1:  $m_0^q, m_0^s \leftarrow \mathcal{Q}_m(0)$
- 2:  $v_0^q, v_0^s \leftarrow \mathcal{Q}_v(0)$
- 3:  $\theta'_0, \rho_0 \leftarrow \mathcal{C}(\theta_0)$
- 4: Initialize  $t \leftarrow 0$
- 5: **while** not converged **do**
- 6:    $t \leftarrow t + 1$
- 7:    $B_t \sim \mathcal{B}$
- 8:    $g_t \leftarrow \nabla_{\theta} \mathcal{L}(B_t; \theta'_{t-1})$
- 9:   // Reconstruct optimizer state and master weight
- 10:    $m_{t-1} \leftarrow \mathcal{Q}_m^{-1}(m_{t-1}^q, m_{t-1}^s)$
- 11:    $v_{t-1} \leftarrow \mathcal{Q}_v^{-1}(v_{t-1}^q, v_{t-1}^s)$
- 12:    $\theta_{t-1} \leftarrow \mathcal{C}^{-1}(\theta'_{t-1}, \rho_{t-1})$
- 13:   // Standard optimizer update
- 14:    $m_t \leftarrow \beta_1 m_{t-1} + (1 - \beta_1) g_t$
- 15:    $v_t \leftarrow \beta_2 v_{t-1} + (1 - \beta_2) g_t^2$
- 16:    $\hat{m}_t \leftarrow m_t / (1 - \beta_1^t)$
- 17:    $\hat{v}_t \leftarrow v_t / (1 - \beta_2^t)$
- 18:    $\theta_t \leftarrow \theta_{t-1} - \eta_t (\hat{m}_t / (\sqrt{\hat{v}_t} + \varepsilon) + \lambda \theta_{t-1})$
- 19:   // Quantize optimizer state and split master weight
- 20:    $m_t^q, m_t^s \leftarrow \mathcal{Q}_m(m_t)$
- 21:    $v_t^q, v_t^s \leftarrow \mathcal{Q}_v(v_t)$
- 22:    $\theta'_t, \rho_t \leftarrow \mathcal{C}(\theta_t)$

### 3.3. Optimizer Update

We modify any given gradient update rule by adding a prologue and an epilogue. In the prologue, we dequantize the optimizer states and reconstruct the master weight  $\theta$  from the low-precision weight  $\theta'$  and the error correction bits  $\rho$ . In the epilogue, we quantize the new optimizer state and split the new  $\theta$  into an updated  $(\theta', \rho)$ . At the start of training, we downcast the master weights to BF16 to ensure training runs directly on the low-precision  $\theta'$  with no downcasts apart from our optimizer step. Algorithm 4 illustrates these changes for the AdamW optimizer, and Algorithms 5 and 6 in the appendix show the corresponding changes to SGD and Lion respectively.

### 3.4. Implementation

**Update kernels.** Since compression and quantization are bandwidth-bound operations, we implement the optimizer step as a single fused Triton kernel (Tillet et al., 2019). For example, for the AdamW update our kernel encompasses steps 9 through 22 from Algorithm 4.

**Gradient release.** We implement gradient release (Zhang et al., 2023), interleaving gradient computation with opti-

mizer updates during backpropagation. As each gradient is computed, we eagerly apply the optimizer rule to free the gradient memory. We apply this optimization only when gradient accumulation is disabled.

**Distributed training.** Our implementation is compatible with parameter sharding approaches such as PyTorch FSDP (Zhao et al., 2023). During forward and backward passes, only the 16-bit  $\theta'$  parameters are all-gathered; the correction term  $\rho$  remains local with the optimizer states.

**Checkpoint size.** Our representation reduces checkpoint size. For instance, standard Adam checkpoints require 12 bytes per parameter (4 for weights, 4 for momentum, 4 for variance); FlashAdamW requires only 5 bytes (2 for weights, 1 for correction, 1 for momentum, and 1 for variance). For a 7B model, checkpoint size reduces from 84GB to 35GB.

**Code availability.** We make our implementation widely available as an open-source PyTorch library at <https://github.com/databricks/flashtoptim>.

## 4. Experiments

### 4.1. Experimental Setup

We evaluate FlashOptim with three optimizers: SGD with momentum (Polyak, 1964), AdamW (Loshchilov and Hutter, 2017), and Lion (Chen et al., 2023). We refer to these variants as FlashSGD, FlashAdamW, and FlashLion. We test these across several large-scale deep learning tasks, including image classification, language model pretraining, and supervised finetuning.

To ensure a fair comparison, all experiments use identical hyperparameters between reference optimizers and their FlashOptim counterparts. We re-implement the reference optimizers with similar fused Triton kernels for consistent measurement of memory and throughput, and all reference implementations use mixed precision (Micikevicius et al., 2018) to keep activations in 16-bit precision. The precisions of master weights  $\theta$ , error correction term  $\rho$ , gradients  $g$ , momentum  $m$ , variance  $v$ , and activations  $a$  are as follows:

	$\theta$	$\rho$	$g$	$m$	$v$	$a$
Reference	FP32	—	FP32	FP32	FP32	BF16
FlashOptim	BF16	INT8	BF16	INT8	UINT8	BF16

Our experiments demonstrate four main findings. First, FlashOptim matches reference convergence and accuracy across all tested configurations (§4.2). Second, it reduces optimizer memory by over 50% with negligible computational overhead (§4.3). Third, our ULP-based weight splitting achieves near-optimal reconstruction (§4.4). Finally, our companding functions significantly reduce quantization error for both momentum and variance states (§4.5).

**Image Classification.** We train a ResNet-50 architecture (He et al., 2016b) on the ILSVRC2012 (ImageNet-1K)

Table 2: **Image Classification & LLM Finetuning Results.** Validation accuracy for ResNet-50 (first two columns), and GSM8k accuracy for the LLM finetuning task (last column). We report standard deviation across 3 training runs. In all settings FlashOptim matches the reference scores.

	ImageNet Top-1 Acc.		GSM8k Acc.
	SGD	AdamW	AdamW
Reference	77.01 ± 0.02	75.51 ± 0.09	75.09 ± 0.40
FlashOptim	77.16 ± 0.09	75.67 ± 0.04	74.98 ± 0.77

dataset (Deng et al., 2009). We use the hyperparameters recommended by Nvidia (NVIDIA, 2023), with additional details provided in Appendix B.1.

**LLM Pretraining.** We evaluate LLM pretraining using the training recipe outlined in the nanoGPT repository (Karpathy, 2023). We use the GPT-2 (Radford et al., 2019) architecture and train on a 10B token subset of the FineWeb dataset (Penedo et al., 2024), following the setup of Jordan (2024). We provide hyperparameter details in Appendix B.2. We evaluate models using a suite of in-context learning (ICL) benchmarks that assess commonsense reasoning and language understanding capabilities. We provide a complete list of benchmarks in Appendix B.3.

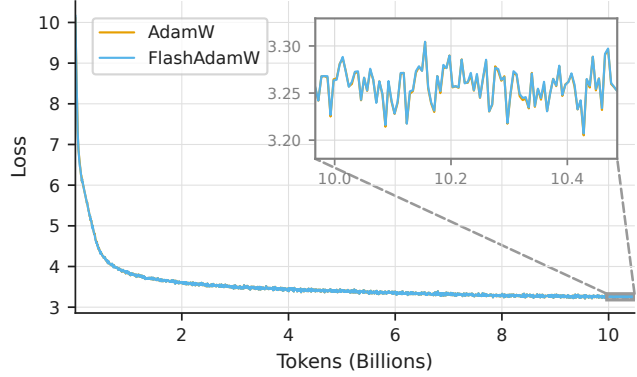
**LLM Finetuning.** We run supervised finetuning on a pretrained Llama-3.1-8B model (Dubey et al., 2024) on OpenMathInstruct-2 (Toshniwal et al., 2024), and evaluate on the GSM8k (Cobbe et al., 2021) benchmark. We provide further hyperparameter details in Appendix B.4.

**Training and Infrastructure.** We train with distributed data parallelism for the image classification and LLM pre-training tasks, and for LLM finetuning we use FSDP (Zhao et al., 2023) and activation checkpointing. We train all models using PyTorch 2.8 and CUDA 12.8 on NVIDIA H100 GPUs. We report the mean and standard deviation for all our results with 3 random seeds. For loss curve comparisons, we use identical data ordering across methods. System metrics (memory, timing) are measured in steady-state.

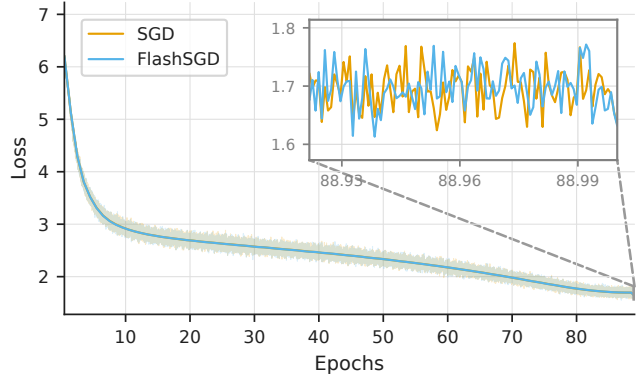
## 4.2. Convergence and Accuracy

We first verify that FlashOptim introduces no measurable degradation by comparing training convergence and validation accuracy. Figure 2a shows training loss for LLM pre-training with AdamW and FlashAdamW. FlashAdamW produces a nearly identical trajectory to the reference AdamW and closely tracks AdamW even after 20,000 parameter updates, indicating that reduced precision does not affect learning dynamics. Figure 2b shows similar results for image classification: FlashSGD matches reference SGD throughout training. For LLM finetuning, Figure 8 in the appendix shows an analogous result for AdamW.

Table 2 reports final scores for the image classification



(a) LLM Pretraining (GPT-2 + AdamW)



(b) Vision Classification (ResNet-50 + SGD)

Figure 2: **Training convergence.** Comparison of training loss trajectories between reference optimizers and their FlashOptim variants. Both achieve nearly identical loss curves throughout training, demonstrating that our memory optimizations do not impact model quality.

and LLM finetuning tasks. FlashSGD and FlashAdamW match the reference optimizer scores in all three settings. Table 3 compares final validation loss and in-context learning scores for the LLM pretraining task. Models trained with FlashOptim achieve scores within variance of reference optimizers across all metrics.

## 4.3. Memory and Speed

We compare memory requirements and optimizer step time, demonstrating that FlashOptim reduces peak memory (PyTorch Contributors, 2025) without practical overhead. We focus on parameter-related memory (weights, optimizer state, gradients) since activation memory is identical across both settings. To isolate contributions, we ablate: weight splitting (Weight Split) with full-precision optimizer states, and optimizer state quantization with companding (Opt. Quant.) with FP32 master weights.

Table 4 breaks down the memory usage for LLM finetuning on a Llama-3.1-8B model. As anticipated, we reduce

Table 3: **LLM Pretraining Results.** NanoGPT results with GPT-2 (124M). We report validation loss and accuracy (%) on in-context learning benchmarks assessing commonsense reasoning and language understanding. We report standard deviation across 3 training runs.

Optimizer	Val Loss	HellaSwag	ARC-E	CSQA	PIQA	LAMBADA	Winograd	BoolQ	Mean ICL
AdamW	3.263 ± 0.001	31.9 ± 0.2	39.6 ± 0.7	25.9 ± 4.1	64.3 ± 0.0	31.0 ± 1.2	57.3 ± 0.6	58.1 ± 3.6	<b>44.0 ± 0.4</b>
FlashAdamW	3.265 ± 0.001	31.9 ± 0.5	39.5 ± 0.9	30.8 ± 2.1	64.5 ± 0.3	31.9 ± 0.7	59.1 ± 1.1	57.2 ± 4.8	<b>45.0 ± 1.0</b>
Lion	3.240 ± 0.002	32.3 ± 0.0	40.0 ± 0.5	23.3 ± 1.8	63.8 ± 1.0	31.5 ± 0.2	58.9 ± 2.0	58.1 ± 2.4	<b>44.0 ± 0.5</b>
FlashLion	3.240 ± 0.001	32.4 ± 0.3	40.8 ± 0.2	25.4 ± 2.9	64.2 ± 0.5	31.6 ± 0.5	59.1 ± 2.4	59.1 ± 2.3	<b>44.7 ± 0.5</b>

Table 4: **Profiling.** Runtime measurements for LLM Finetuning with Llama-3.1-8B. We capture master weight memory (Params), optimizer state memory (Optim), peak GPU memory (Peak), and optimizer step times (Step).

Variant	Params		Optim		Peak		Step
	GiB	Δ	GiB	Δ	GiB	Δ	ms
Reference	29.9		59.8		175.2		12.5
FlashOptim	<b>15.0</b>	-50%	<b>23.4</b>	-61%	<b>112.9</b>	-36%	11.5
<i>Ablations</i>							
Weight Split	15.0	-50%	67.3	+12%	156.7	-11%	10.7
Opt. Quant.	29.9		15.9	-73%	131.4	-25%	10.5

parameter memory by 50% from dropping precision from FP32 to BF16, and reduce optimizer memory by 60% from quantizing the optimizer state tensors. Moreover, when looking at peak memory (including activations), FlashOptim reduces it by 36% with no practical slowdown in optimizer step times.

Ablating each component confirms that weight splitting halves master weight memory while adding 12% of extra optimizer state. Optimizer state quantization reduces optimizer state by  $\sim 73\%$  by mapping FP32 tensors to INT8/UINT8; the reduction is slightly less than 75% due to the overhead of storing FP16 scale factors for each group of 32 elements. Tables 6 and 8 in the appendix show similar trends for LLM pretraining and image classification.

#### 4.4. Weight Error Correction

We compare our weight splitting scheme to Zamirai et al. (2020), who store the rounding error in a floating-point buffer for Kahan summation error correction. Since both approaches are data-independent, we evaluate them exhaustively over all finite FP32 bitstrings, computing relative error after applying compression and decompression in sequence. We consider four methods: a no error correction baseline, storing error in the same 16-bit format, our ULP-normalized error with 8-bit integers, and ours with 16-bit integers.

Figure 3 plots mean relative error versus exponent for BF16 and FP16. For BF16, our ULP approach with 16-bit correction achieves near-zero error ( $< 10^{-9}$ ). With 16 bits of

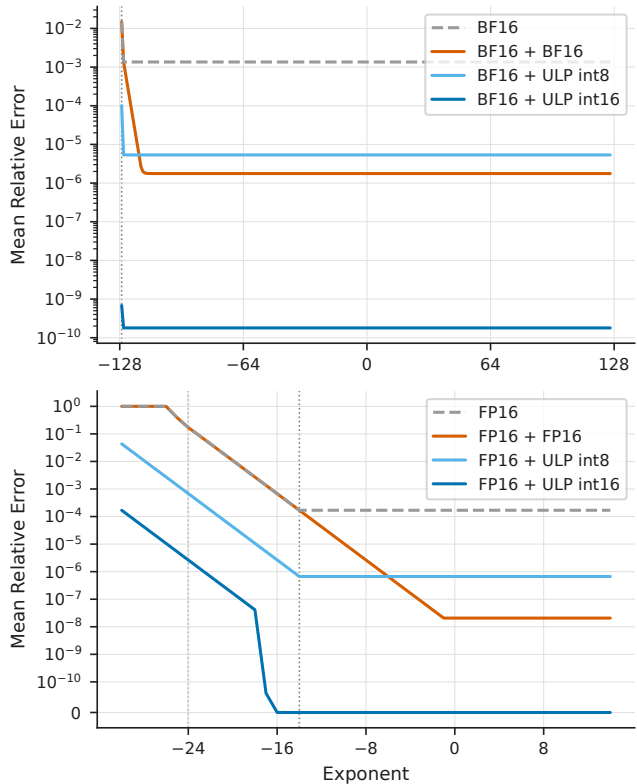


Figure 3: **FP32 Reconstruction Error.** Comparison of FP32 reconstruction error for different weight compression schemes across exponent ranges for a target datatype of BF16 (top) and FP16 (bottom). Our ULP-based error correction achieves lower relative error particularly for small exponents. Denormal floating point ranges are indicated with vertical dotted lines.

correction term, we achieve perfect bitwise reconstruction in 99.92% of the values. In contrast, storing the error in BF16 (BF16+BF16) produces substantially worse error ( $> 10^{-6}$ ), comparable to our 24-bit format. For FP16, our 32-bit ULP format perfectly reconstructs values in the normal range and dominates FP16+FP16 throughout. Our 24-bit format produces constant error across the normal range, improving worst-case error from  $10^{-4}$  to under  $10^{-6}$ .

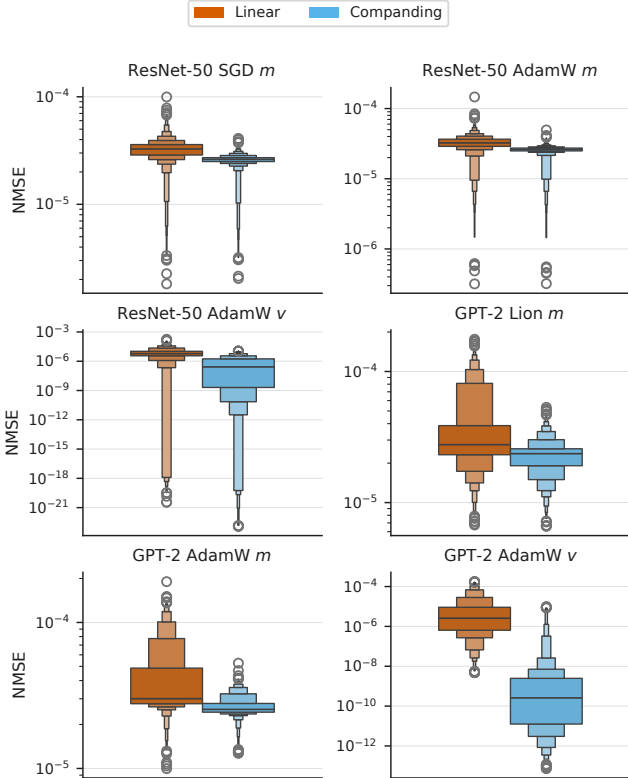


Figure 4: **Optimizer state quantization error.** NMSE comparison between standard scaled integer quantization (Linear) and our companding approach for momentum ( $m$ ) and variance ( $v$ ) buffers across different optimizers and datasets. Companding reduces quantization error across all optimizer types and tensor types, with particularly large improvements for variance tensors.

#### 4.5. Optimizer State Quantization

We validate our companding functions by comparing quantization error against standard scaled integer quantization. Using a fixed full precision training trajectory for consistency, we quantize and dequantize momentum and variance buffers at each step, computing normalized MSE (NMSE) against the original values. Figure 4 shows quantile distributions of NMSE for each optimizer and buffer type. Companding reduces error for momentum buffers and provides substantial improvements for variance buffers, where NMSE drops significantly.

Beyond reducing quantization error, in some cases companding is essential for training stability. Figure 5 shows LLM pretraining with and without variance companding: linear quantization causes training to diverge, while companding maintains stable convergence.

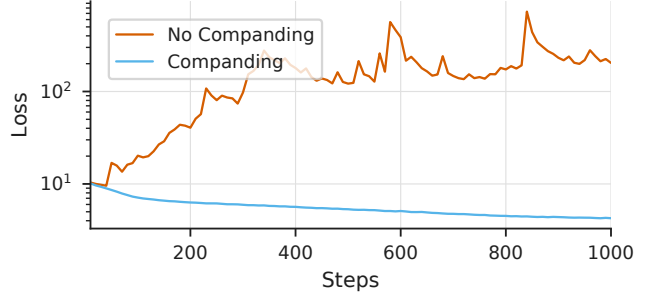


Figure 5: **Companding prevents training divergence.** GPT-2 training with AdamW and quantized optimizer states: linear quantization (no companding) causes rapid divergence, while our companding approach maintains stable training dynamics.

## 5. Limitations

FlashOptim is designed to minimize parameter-associated memory consumption, so models with large parameter counts and small activations benefit most from our optimizations. Smaller architectures with large activations, such as convolutional networks with high-resolution feature maps, are often dominated by activation memory. In these activation-dominated regimes, a 50% reduction in parameter memory translates to modest total memory savings and techniques like activation checkpointing are more effective for such workloads.

Another limitation is that some tasks and architectures may be more sensitive to quantization than those in our benchmarks. The effectiveness of a quantization pipeline depends on the data distribution, and there is no guarantee that our method (or any quantization approach) will preserve model quality in all cases. Consequently, our implementation allows selectively disabling compression or excluding specific layers as needed.

Finally, while we find that 24-bit master weights are sufficient in our experiments, not even 32 bits are guaranteed to suffice in all cases. Successive (normal) floating-point values differ by a factor of roughly  $2^{-\text{num\_mantissa\_bits}}$ , and if the ratio of weight update to weight magnitude falls below this threshold, the update will be discarded.

## 6. Conclusion

We introduced FlashOptim, a method to reduce the memory footprint of neural network training while preserving optimizer semantics and model quality. FlashOptim provides drop-in replacements for common optimizers and requires no additional tuning.

Our approach combines two key techniques. First, we reduce master weights from 32 to 24 bits via improved floating point error correction. Second, we use companding func-

tions to enable 8-bit optimizer state quantization. Together with 16-bit gradients, these reduce per-parameter memory by over 50% for AdamW.

We validated FlashOptim on image and language benchmarks using SGD, AdamW, and Lion. Across all settings, our method matches reference implementations in both loss and accuracy while providing significant memory savings. FlashOptim composes with FSDP and activation checkpointing, enabling multiplicative benefits for large-scale training. By lowering memory requirements, FlashOptim enables practitioners and researchers with limited hardware to train larger models than previously feasible.

## Acknowledgements

We are grateful to Jonathan Frankle, Xing Chen, and Matei Zaharia for their continued support and guidance. We also thank Jialu Liu and Erich Elsen for insightful discussions.

## References

- Rohan Anil, Vineet Gupta, Tomer Koren, and Yoram Singer. Memory-efficient adaptive optimization. In *Advances in Neural Information Processing Systems (NeurIPS)*, 2019. 3
- Dan Biderman, Jacob Portes, Jose Javier Gonzalez Ortiz, Mansheej Paul, Philip Greengard, Connor Jennings, Daniel King, Sam Havens, Vitaliy Chiley, Jonathan Frankle, et al. Lora learns less and forgets less. *arXiv preprint arXiv:2405.09673*, 2024. 1
- Yonatan Bisk, Rowan Zellers, Ronan Le Bras, Jianfeng Gao, and Yejin Choi. Piqa: Reasoning about physical commonsense in natural language. In *Proceedings of the AAAI Conference on Artificial Intelligence*, volume 34, pages 7432–7439, 2020. 14
- Tom Brown, Benjamin Mann, Nick Ryder, Melanie Subbiah, Jared D Kaplan, Prafulla Dhariwal, Arvind Neelakantan, Pranav Shyam, Girish Sastry, Amanda Askell, et al. Language models are few-shot learners. *Advances in neural information processing systems*, 33:1877–1901, 2020. 14
- Tianqi Chen, Bing Xu, Chiyuan Zhang, and Carlos Guestrin. Training deep nets with sublinear memory cost. *arXiv preprint arXiv:1604.06174*, 2016. 3, 15
- Xiangning Chen, Chen Liang, Da Huang, Esteban Real, Kaiyuan Wang, Yao Liu, Hieu Pham, Xuanyi Dong, Thang Luong, Chou-Jui Hsieh, Yifeng Lu, and Quoc V. Le. Symbolic discovery of optimization algorithms. In *Advances in Neural Information Processing Systems (NeurIPS)*, 2023. 3, 5
- Aakanksha Chowdhery, Sharan Narang, Jacob Devlin, Maarten Bosma, Gaurav Mishra, Adam Roberts, Paul Barham, Hyung Won Chung, Charles Sutton, Sebastian Gehrmann, et al. PaLM: Scaling language modeling with pathways. *Journal of Machine Learning Research*, 24(240):1–113, 2023. 1
- Christopher Clark, Kenton Lee, Ming-Wei Chang, Tom Kwiatkowski, Michael Collins, and Kristina Toutanova. Boolq: Exploring the surprising difficulty of natural yes/no questions. In *Proceedings of the Conference of the North American Chapter of the Association for Computational Linguistics (NAACL)*, pages 2924–2936, 2019. 15
- Peter Clark, Isaac Cowhey, Oren Etzioni, Tushar Khot, Ashish Sabharwal, Carissa Schoenick, and Oyvind Tafjord. Think you have solved question answering? try arc, the ai2 reasoning challenge. *arXiv preprint arXiv:1803.05457*, 2018. 14
- Karl Cobbe, Vineet Kosaraju, Mohammad Bavarian, Mark Chen, Heewoo Jun, Lukasz Kaiser, Matthias Plappert, Jerry Tworek, Jacob Hilton, Reiichiro Nakano, Christopher Hesse, and John Schulman. Training verifiers to solve math word problems. *arXiv preprint arXiv:2110.14168*, 2021. 6, 15
- Mostafa Dehghani, Josip Djolonga, Basil Mustafa, Piotr Padlewski, Jonathan Heek, Justin Gilmer, Andreas Peter Steiner, Mathilde Caron, Robert Geirhos, Ibrahim Alabdulmohsin, et al. Scaling vision transformers to 22 billion parameters. In *International Conference on Machine Learning*, pages 7480–7512. PMLR, 2023. 1
- Jia Deng, Wei Dong, Richard Socher, Li-Jia Li, Kai Li, and Li Fei-Fei. Imagenet: A large-scale hierarchical image database. In *2009 IEEE conference on computer vision and pattern recognition*, pages 248–255. Ieee, 2009. 6, 13
- Tim Dettmers, Mike Lewis, Sam Shleifer, and Luke Zettlemoyer. 8-bit optimizers via block-wise quantization. In *International Conference on Learning Representations (ICLR)*, 2022. 2, 4
- Tim Dettmers, Artidoro Pagnoni, Ari Holtzman, and Luke Zettlemoyer. QLoRA: Efficient finetuning of quantized llms. *Advances in neural information processing systems*, 36:10088–10115, 2023. 3
- Abhimanyu Dubey, Abhinav Jauhri, Abhinav Pandey, Abhishek Kadian, Ahmad Al-Dahle, Aiesha Letman, Akhil Mathur, Alan Schelten, Amy Yang, Angela Fan, et al. The llama 3 herd of models. *arXiv preprint arXiv:2407.21783*, 2024. 6, 15
- Wei Feng, Will Constable, and Yifan Mao. Getting started with fully sharded data parallel (FSDP2). PyTorch Tutorials, 2022. URL [https://docs.pytorch.org/tutorials/intermediate/FSDP\\_tutorial.html](https://docs.pytorch.org/tutorials/intermediate/FSDP_tutorial.html). Last updated: Sep 02, 2025. Accessed: Jan 28, 2026. 15
- Maxim Fishman, Brian Chmiel, Ron Banner, and Daniel Soudry. Scaling FP8 training to trillion-token LLMs. In *International Conference on Learning Representations (ICLR)*, 2025. Spotlight. 2
- Boris Ginsburg, Patrice Castonguay, Oleksii Hrinchuk, Oleksii Kuchaiev, Vitaly Lavrukhin, Ryan Leary, Jason Li, Huyen Nguyen, Yang Zhang, and Jonathan M Cohen. Stochastic gradient methods with layer-wise adaptive moments for training of deep networks. *arXiv preprint arXiv:1905.11286*, 2019. 3

- David Goldberg. What every computer scientist should know about floating-point arithmetic. *ACM computing surveys (CSUR)*, 23 (1):5–48, 1991. 3
- Google. Bfloat16: The secret to high performance on cloud tpus. Google Cloud Blog, August 2019. 2
- Priya Goyal, Piotr Dollár, Ross Girshick, Pieter Noordhuis, Lukasz Wesolowski, Aapo Kyrola, Andrew Tulloch, Yangqing Jia, and Kaiming He. Accurate, large minibatch sgd: Training imagenet in 1 hour. *arXiv preprint arXiv:1706.02677*, 2017. 13
- Kaiming He, Xiangyu Zhang, Shaoqing Ren, and Jian Sun. Identity mappings in deep residual networks. In *European conference on computer vision*, pages 630–645. Springer, 2016a. 13
- Kaiming He, Xiangyu Zhang, Shaoqing Ren, and Jian Sun. Deep residual learning for image recognition. In *Proceedings of the IEEE Conference on Computer Vision and Pattern Recognition (CVPR)*, pages 770–778, 2016b. 5, 13
- Jordan Hoffmann, Sebastian Borgeaud, Arthur Mensch, Elena Buchatskaya, Trevor Cai, Eliza Rutherford, Diego de Las Casas, Lisa Anne Hendricks, Johannes Welbl, Aidan Clark, et al. Training compute-optimal large language models. *arXiv preprint arXiv:2203.15556*, 2022. 1
- Edward J. Hu, Yelong Shen, Phillip Wallis, Zeyuan Allen-Zhu, Yuanzhi Li, Shean Wang, Lu Wang, and Weizhu Chen. LoRA: Low-rank adaptation of large language models. In *International Conference on Learning Representations (ICLR)*, 2022. 1, 3
- Keller Jordan. modded-nanogpt: Speedrunning the nanogpt baseline. <https://github.com/KellerJordan/modded-nanogpt>, 2024. 6
- Keller Jordan, Yuchen Jin, Vlado Boza, Jiacheng You, Franz Cesta, Laker Newhouse, and Jeremy Bernstein. Muon: An optimizer for hidden layers in neural networks, 2024. URL <https://kellerjordan.github.io/posts/muon/>. 3
- Florian Kainz, Rod Bogart, and Drew Hess. The OpenEXR image file format. In Randima Fernando, editor, *GPU Gems: Programming Techniques, Tips and Tricks for Real-Time Graphics*, chapter 26, pages 425–444. Addison-Wesley, 2004. 4
- Dhiraj Kalamkar, Dheevatsa Mudigere, Naveen Mellempudi, Dipankar Das, Kunal Banerjee, Sasikanth Avancha, Dharma Teja Vooturi, Nataraj Jammalamadaka, Jianyu Huang, Hector Yuen, et al. A study of bfloat16 for deep learning training. *arXiv preprint arXiv:1905.12322*, 2019. 2
- Jared Kaplan, Sam McCandlish, Tom Henighan, Tom B Brown, Benjamin Chess, Rewon Child, Scott Gray, Alec Radford, Jeffrey Wu, and Dario Amodei. Scaling laws for neural language models. *arXiv preprint arXiv:2001.08361*, 2020. 1
- Andrej Karpathy. nanogpt. <https://github.com/karpathy/nanoGPT>, 2023. 6
- kjj0. fineweb10b-gpt2. Hugging Face Datasets, 2024. URL <https://huggingface.co/datasets/kjj0/fineweb10b-gpt2>. GPT-2 tokenized version of fineweb10B. Accessed: Jan 28, 2026. 14
- Vijay Anand Korthikanti, Jared Casper, Sangkug Lym, Lawrence McAfee, Michael Andersch, Mohammad Shoeybi, and Bryan Catanzaro. Reducing activation recomputation in large transformer models. *Proceedings of Machine Learning and Systems*, 5:341–353, 2023. 3
- Alex Krizhevsky, Ilya Sutskever, and Geoffrey E Hinton. Imagenet classification with deep convolutional neural networks. *Advances in neural information processing systems*, 25, 2012. 13
- Hector J. Levesque, Ernest Davis, and Leora Morgenstern. The winograd schema challenge. In *Proceedings of the Thirteenth International Conference on the Principles of Knowledge Representation and Reasoning (KR)*, pages 552–561, 2012. 15
- Bingrui Li, Jianfei Chen, and Jun Zhu. Memory efficient optimizers with 4-bit states. *Advances in Neural Information Processing Systems*, 36:15136–15171, 2023. 2
- Xiang Lisa Li and Percy Liang. Prefix-tuning: Optimizing continuous prompts for generation. *arXiv preprint arXiv:2101.00190*, 2021. 1
- Jingyuan Liu, Jianlin Su, Xingcheng Yao, Zhejun Jiang, Guokun Lai, Yulun Du, Yidao Qin, Weixin Xu, Enzhe Lu, Junjie Yan, et al. Muon is scalable for llm training. *arXiv preprint arXiv:2502.16982*, 2025. 3
- Ilya Loshchilov and Frank Hutter. Decoupled weight decay regularization. *arXiv preprint arXiv:1711.05101*, 2017. 5
- Kai Lv, Hang Yan, Qipeng Guo, Haijun Lv, and Xipeng Qiu. Adalomo: Low-memory optimization with adaptive learning rate. In *Findings of the Association for Computational Linguistics: ACL 2024*, pages 12486–12502, 2024a. 2
- Kai Lv, Yuqing Yang, Tengxiao Liu, Qinghui Gao, Qipeng Guo, and Xipeng Qiu. Full parameter fine-tuning for large language models with limited resources. In *Proceedings of the 62nd Annual Meeting of the Association for Computational Linguistics (ACL)*, pages 8187–8198, 2024b. 2
- Naveen Mellempudi, Sudarshan Srinivasan, Dipankar Das, and Bharat Kaul. Mixed precision training with 8-bit floating point. *arXiv preprint arXiv:1905.12334*, 2019. 2
- Paulius Micikevicius, Sharan Narang, Jonah Alben, Gregory Diamos, Erich Elsen, David Garcia, Boris Ginsburg, Michael Houston, Oleksii Kuchaiev, Ganesh Venkatesh, and Hao Wu. Mixed precision training. In *International Conference on Learning Representations (ICLR)*, 2018. 2, 3, 5
- Paulius Micikevicius, Dusan Stolic, Neil Burgess, Marius Cornea, Pradeep Dubey, Richard Grisenthwaite, Sangwon Ha, Alexander Heinecke, Patrick Judd, John Kamalu, et al. FP8 formats for deep learning. *arXiv preprint arXiv:2209.05433*, 2022. 2

- Todor Mihaylov, Peter Clark, Tushar Khot, and Ashish Sabharwal. Can a suit of armor conduct electricity? a new dataset for open book question answering. In *Proceedings of the Conference on Empirical Methods in Natural Language Processing (EMNLP)*, pages 2381–2391, 2018. 14
- Ionut-Vlad Modoranu, Mher Safaryan, Grigory Malinovsky, Eldar Kurtić, Thomas Robert, Peter Richtárik, and Dan Alistarh. MicroAdam: Accurate adaptive optimization with low space overhead and provable convergence. *Advances in Neural Information Processing Systems*, 37:1–43, 2024. 2
- MosaicML. Streaming: A data loading library for training on large datasets. <https://github.com/mosaicml/streaming>, 2022. 13
- Saaketh Narayan, Abhay Gupta, Mansheej Paul, and Davis Blalock.  $\mu$ nit Scaling: Simple and scalable FP8 LLM training. *arXiv preprint arXiv:2502.05967*, 2025. 2
- NVIDIA. ResNet v1.5 for PyTorch. [https://catalog.ngc.nvidia.com/orgs/nvidia/resources/resnet\\_50\\_v1\\_5\\_for\\_pytorch](https://catalog.ngc.nvidia.com/orgs/nvidia/resources/resnet_50_v1_5_for_pytorch), 2023. 6
- Denis Paperno, Germán Kruszewski, Angeliki Lazaridou, Quan Ngoc Pham, Raffaella Bernardi, Sandro Pezzelle, Marco Baroni, Gemma Boleda, and Raquel Fernández. The lambda dataset: Word prediction requiring a broad discourse context. In *Proceedings of the 54th Annual Meeting of the Association for Computational Linguistics (ACL)*, pages 1525–1534, 2016. 15
- Guilherme Penedo, Hynek Kydlíček, Loubna Ben Allal, Anton Lozhkov, Margaret Mitchell, Colin Raffel, Leandro Von Werra, and Thomas Wolf. The fineweb datasets: Decanting the web for the finest text data at scale. *arXiv preprint arXiv:2406.17557*, 2024. 6, 14
- Houwen Peng et al. Fp8-lm: Training fp8 large language models. *arXiv preprint arXiv:2310.18313*, 2023. 2
- Thomas Pethick, Wanyun Xie, Kimon Antonakopoulos, Zhenyu Zhu, Antonio Silveti-Falls, and Volkan Cevher. Training deep learning models with norm-constrained Imos. In *International Conference on Machine Learning (ICML)*, 2025. 3
- Boris T Polyak. Some methods of speeding up the convergence of iteration methods. *Ussr computational mathematics and mathematical physics*, 4(5):1–17, 1964. 5
- PyTorch Contributors. torch.cuda.memory.memory\_stats. PyTorch Documentation, 2025. URL [https://docs.pytorch.org/docs/main/generated/torch.cuda.memory.memory\\_stats.html](https://docs.pytorch.org/docs/main/generated/torch.cuda.memory.memory_stats.html). Accessed: Jan 28, 2026. 6
- Alec Radford, Jeffrey Wu, Rewon Child, David Luan, Dario Amodei, Ilya Sutskever, et al. Language models are unsupervised multitask learners. *OpenAI blog*, 1(8):9, 2019. 6, 14
- Samyam Rajbhandari, Jeff Rasley, Olatunji Ruwase, and Yuxiong He. Zero: Memory optimizations toward training trillion parameter models. In *International Conference for High Performance Computing, Networking, Storage and Analysis (SC)*, 2020. 1, 3
- Samyam Rajbhandari, Olatunji Ruwase, Jeff Rasley, Shaden Smith, and Yuxiong He. Zero-infinity: Breaking the gpu memory wall for extreme scale deep learning. In *International Conference for High Performance Computing, Networking, Storage and Analysis (SC)*, 2021. 3
- Jie Ren, Samyam Rajbhandari, Reza Yazdani Aminabadi, Olatunji Ruwase, Shuangyan Yang, Minjia Zhang, Dong Li, and Yuxiong He. {Zero-offload}: Democratizing {billion-scale} model training. In *2021 USENIX Annual Technical Conference (USENIX ATC 21)*, pages 551–564, 2021. 1, 3
- Jonathan S Rosenfeld, Amir Rosenfeld, Yonatan Belinkov, and Nir Shavit. A constructive prediction of the generalization error across scales. *arXiv preprint arXiv:1909.12673*, 2019. 1
- Noam Shazeer and Mitchell Stern. Adafactor: Adaptive learning rates with sublinear memory cost. In *International Conference on Machine Learning (ICML)*, 2018. 3
- Karen Simonyan and Andrew Zisserman. Very deep convolutional networks for large-scale image recognition. *arXiv preprint arXiv:1409.1556*, 2014. 13
- Christian Szegedy, Vincent Vanhoucke, Sergey Ioffe, Jon Shlens, and Zbigniew Wojna. Rethinking the inception architecture for computer vision. In *Proceedings of the IEEE conference on computer vision and pattern recognition*, pages 2818–2826, 2016. 13
- Alon Talmor, Jonathan Herzig, Nicholas Lourie, and Jonathan Berant. Commonsenseqa: A question answering challenge targeting commonsense knowledge. In *Proceedings of the Conference of the North American Chapter of the Association for Computational Linguistics (NAACL)*, pages 4149–4158, 2019. 14
- Mingxing Tan and Quoc Le. Efficientnet: Rethinking model scaling for convolutional neural networks. In *International conference on machine learning*, pages 6105–6114. PMLR, 2019. 1
- Hanlin Tang, Shaoduo Gan, Ammar Ahmad Awan, Samyam Rajbhandari, Conglong Li, Xiangru Lian, Ji Liu, Ce Zhang, and Yuxiong He. 1-bit Adam: Communication efficient large-scale training with Adam’s convergence speed. In *International Conference on Machine Learning (ICML)*, 2021. 2
- Philippe Tillet, H. T. Kung, and David Cox. Triton: An intermediate language and compiler for tiled neural network computations. In *Proceedings of the 3rd ACM SIGPLAN International Workshop on Machine Learning and Programming Languages (MAPL)*, pages 10–19, 2019. 5
- Shubham Toshniwal, Ivan Moshkov, Sean Narenthiran, Daria Gitman, Fei Jia, and Igor Gitman. OpenMathInstruct-2: Accelerating ai for math with massive open-source instruction data. In *Advances in Neural Information Processing Systems (NeurIPS)*, 2024. 6, 15
- Thijs Vogels, Sai Praneeth Karimireddy, and Martin Jaggi. PowerSGD: Practical low-rank gradient compression for distributed optimization. In *Advances in Neural Information Processing Systems (NeurIPS)*, 2019. 2

- Naigang Wang, Jungwook Choi, Daniel Brand, Chia-Yu Chen, and Kailash Gopalakrishnan. Training deep neural networks with 8-bit floating point numbers. *Advances in neural information processing systems*, 31, 2018. 2
- Benjamin Warner. optimi: Fast, modern, and low precision pytorch optimizers. <https://github.com/warner-benjamin/optimi>, 2024. 2, 3
- Haocheng Xi, Han Cai, Ligeng Zhu, Yao Lu, Kurt Keutzer, Jianfei Chen, and Song Han. COAT: Compressing optimizer states and activation for memory-efficient FP8 training. In *International Conference on Learning Representations (ICLR)*, 2025. 2
- Pedram Zamirai, Jian Zhang, Christopher Aberger, and Christopher De Sa. Revisiting bfloat16 training. *arXiv preprint arXiv:2010.06192*, 2020. 2, 3, 7
- Rowan Zellers, Ari Holtzman, Yonatan Bisk, Ali Farhadi, and Yejin Choi. Hellaswag: Can a machine really finish your sentence? In *Proceedings of the 57th Annual Meeting of the Association for Computational Linguistics (ACL)*, pages 4791–4800, 2019. 14
- Yijia Zhang, Yibo Han, Shijie Cao, Guohao Dai, Youshan Miao, Ting Cao, Fan Yang, and Ningyi Xu. Adam accumulation to reduce memory footprints of both activations and gradients for large-scale DNN training. In *European Conference on Artificial Intelligence (ECAI)*, 2023. 2, 5
- Yushun Zhang, Congliang Chen, Ziniu Li, Tian Ding, Chenwei Wu, Yinyu Ye, Zhi-Quan Luo, and Ruoyu Sun. Adam-mini: Use fewer learning rates to gain more. In *International Conference on Learning Representations (ICLR)*, 2025. 3
- Jiawei Zhao, Zhenyu Zhang, Beidi Chen, Zhangyang Wang, Anima Anandkumar, and Yuandong Tian. GaLore: Memory-efficient llm training by gradient low-rank projection. In *International Conference on Machine Learning (ICML)*, 2024a. 3
- Pengxiang Zhao, Ping Li, Yingjie Gu, Yi Zheng, Stephan Ludger Kölker, Zhefeng Wang, and Xiaoming Yuan. Adapprox: Adaptive approximation in Adam optimization via randomized low-rank matrices. *arXiv preprint arXiv:2403.14958*, 2024b. 3
- Yanli Zhao, Andrew Gu, Rohan Varma, Liang Luo, Chien-Chin Huang, Min Xu, Less Wright, Hamid Shojanazeri, Myle Ott, Sam Shleifer, Alban Desmaison, Can Balioglu, Pritam Damania, Bernard Nguyen, Geeta Chauhan, Yuchen Hao, Ajit Mathews, and Shen Li. Pytorch fsdp: Experiences on scaling fully sharded data parallel. *Proceedings of the VLDB Endowment (PVLDB)*, 16(12):3848–3860, 2023. doi: 10.14778/3611540.3611569. 3, 5, 6
- Hanqing Zhu, Zhenyu Zhang, Wenyan Cong, Xi Liu, Sem Park, Vikas Chandra, Bo Long, David Z. Pan, Zhangyang Wang, and Jinwon Lee. APOLLO: Sgd-like memory, adamw-level performance. In *Proceedings of Machine Learning and Systems (MLSys)*, 2025. 3

## A. Method Details

This section provides detailed pseudocode for the FlashOptim version of SGD (Algorithm 5) and Lion (Algorithm 6).

**Algorithm 5** FlashSGD: Memory-Efficient SGD. We highlight the changes from SGD.

**Require:** Parameters  $\theta_0$ , learning rate schedule  $\{\eta_t\}_{t=1}^T$ , momentum  $\mu \in [0, 1)$ , weight decay  $\lambda \geq 0$ , loss  $\mathcal{L}(\theta)$ , minibatch sampler  $\mathcal{B}(\cdot)$

- 1:  $m_0^q, m_0^s \leftarrow \mathcal{Q}_m(0)$
- 2:  $\theta'_0, \rho_0 \leftarrow \mathcal{C}(\theta_0)$
- 3: Initialize  $t \leftarrow 0$
- 4: **while** not converged **do**
- 5:    $t \leftarrow t + 1$
- 6:    $B_t \sim \mathcal{B}$
- 7:    $g_t \leftarrow \nabla_{\theta} \mathcal{L}(B_t; \theta'_{t-1})$
- 8:    $m_{t-1} \leftarrow \mathcal{Q}_m^{-1}(m_{t-1}^q, m_{t-1}^s)$
- 9:    $m_t \leftarrow \mu m_{t-1} + g_t$
- 10:    $m_t^q, m_t^s \leftarrow \mathcal{Q}_m(m_t)$
- 11:    $\theta_{t-1} \leftarrow \mathcal{C}^{-1}(\theta'_{t-1}, \rho_{t-1})$
- 12:    $\theta_t \leftarrow \theta_{t-1} - \eta_t(m_t + \lambda \theta_{t-1})$
- 13:    $\theta'_t, \rho_t \leftarrow \mathcal{C}(\theta_t)$

**Algorithm 6** FlashLion: Memory-Efficient Lion. We highlight the changes from Lion.

**Require:** Parameters  $\theta_0$ , learning rate schedule  $\{\eta_t\}_{t=1}^T$ ,  $\beta_1, \beta_2 \in [0, 1)$ , weight decay  $\lambda \geq 0$ , loss  $\mathcal{L}(\theta)$ , minibatch sampler  $\mathcal{B}(\cdot)$

- 1:  $m_0^q, m_0^s \leftarrow \mathcal{Q}_m(0)$
- 2:  $\theta'_0, \rho_0 \leftarrow \mathcal{C}(\theta_0)$
- 3: Initialize  $t \leftarrow 0$
- 4: **while** not converged **do**
- 5:    $t \leftarrow t + 1$
- 6:    $B_t \sim \mathcal{B}$
- 7:    $g_t \leftarrow \nabla_{\theta} \mathcal{L}(B_t; \theta'_{t-1})$
- 8:    $m_{t-1} \leftarrow \mathcal{Q}_m^{-1}(m_{t-1}^q, m_{t-1}^s)$
- 9:    $u_t \leftarrow \text{sign}(\beta_1 m_{t-1} + (1 - \beta_1) g_t)$
- 10:    $m_t \leftarrow \beta_2 m_{t-1} + (1 - \beta_2) g_t$
- 11:    $m_t^q, m_t^s \leftarrow \mathcal{Q}_m(m_t)$
- 12:    $\theta_{t-1} \leftarrow \mathcal{C}^{-1}(\theta'_{t-1}, \rho_{t-1})$
- 13:    $\theta_t \leftarrow \theta_{t-1} - \eta_t(u_t + \lambda \theta_{t-1})$
- 14:    $\theta'_t, \rho_t \leftarrow \mathcal{C}(\theta_t)$

## B. Experimental Details

For all our experiments we use the MosaicML Streaming (MosaicML, 2022) library to ensure deterministic data loading for distributed training.

## B.1. Image Classification

We train the ResNet-50 (He et al., 2016b) model using the timm library on the ILSVRC2012 (ImageNet-1K) dataset (Deng et al., 2009), which contains approximately 1.28 million training images and 50,000 validation images across 1,000 classes. Our implementation of ImageNet follows the standard setup from (Krizhevsky et al., 2012; Simonyan and Zisserman, 2014). The image is resized with its shorter side randomly sampled in [256, 480] for scale augmentation (Simonyan and Zisserman, 2014). A 224 × 224 crop is randomly sampled from an image or its horizontal flip, and then normalized. For evaluation, the image is first resized to 256 × 256, followed by a 224 × 224 center crop, and then normalized. We initialize the network with Kaiming He initialization (He et al., 2016a) and zero-init residuals (He et al., 2016b).

We train for 90 epochs with a batch size of 1024, using a 5-epoch linear warmup followed by cosine learning rate decay, following the recommended settings from (Goyal et al., 2017). We disable weight-decay for biases and BatchNorm layers. We apply label smoothing (Szegedy et al., 2016) with coefficient 0.1. Both reference (FP32 master weights) and FlashOptim use BF16 activations. Table 5 summarizes the hyperparameters we use for training.

Table 5: Optimizer hyperparameters for ImageNet/ResNet-50.

	SGD	AdamW
Learning Rate	1.024	$3 \times 10^{-3}$
Momentum / Betas	0.9	(0.9, 0.999)
Weight Decay	$3 \times 10^{-5}$	$3 \times 10^{-4}$

**Memory and Speed Profiling.** Table 6 presents the results of the memory and speed profile for training.

Table 6: Memory and speed profiling for image classification (ResNet-50).

Variant	Params		Optim		Total		Step
	GiB	$\Delta$	GiB	$\Delta$	GiB	$\Delta$	ms
<b>SGD</b>							
Reference	0.10		0.10		0.30		8.4
FlashOptim	0.05	-46%	0.05	-45%	0.17	-45%	9.0
Weight Split	0.05	-46%	0.12	+23%	0.23	-22%	8.7
Opt. Quant.	0.10		0.03	-73%	0.23	-23%	8.7
<b>AdamW</b>							
Reference	0.10		0.19		0.40		11.9
FlashOptim	0.05	-46%	0.08	-56%	0.20	-50%	12.2
Weight Split	0.05	-46%	0.21	+11%	0.33	-17%	12.1
Opt. Quant.	0.10		0.05	-73%	0.25	-36%	12.6

Figure 6 shows training loss for ResNet-50 with AdamW and FlashAdamW. FlashAdamW produces a nearly identical trajectory to the reference AdamW implementation.

### B.2. LLM Pretraining

We train the GPT-2 (Radford et al., 2019) (124M) architecture with 12 transformer layers, 12 attention heads, embedding dimension 768, and context length of 1024. We train on the FineWeb10B (kjj0, 2024) dataset, a subset of approximately 10 billion tokens from the FineWeb (Penedo et al., 2024) dataset, tokenized using the GPT-2 BPE tokenizer. We train for 20,000 steps with a batch size of roughly 0.5 million tokens per step. We apply learning rate warmup for the first 700 steps, followed by a cosine decay to 0. The global norm is clipped at 1.0 and a weight decay of 0.1 is used. Weight decay is applied only to 2D parameters (i.e., weight matrices and embeddings), excluding biases and layer normalization parameters. We train in BF16 mixed precision. Table 7 summarizes the optimizer hyperparameters.

Table 7: Optimizer hyperparameters for GPT-2 124M pretraining.

	AdamW	Lion
Learning Rate	$6 \times 10^{-4}$	$2 \times 10^{-4}$
Betas	(0.9, 0.95)	(0.9, 0.95)

**Memory and Speed Profiling.** Table 8 presents the memory and speed profiling results for LLM pretraining.

Figure 7 shows training loss for LLM pretraining with Lion and FlashLion. FlashLion produces a nearly identical trajectory to the reference Lion implementation and closely tracks Lion even after 20,000 parameter updates.

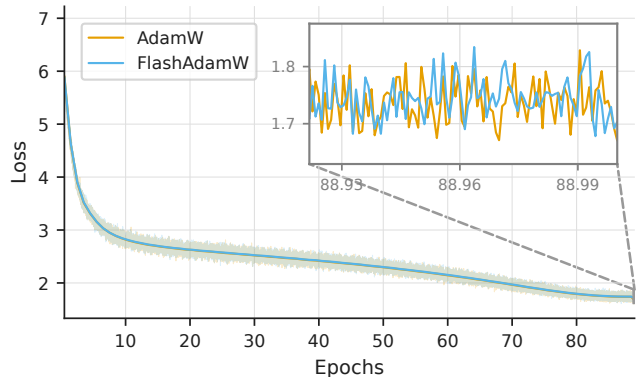


Figure 6: **Training convergence for image classification** (ResNet-50 + AdamW). Comparison of validation accuracy between reference AdamW and FlashAdamW on ImageNet.

Table 8: Memory and speed profiling for LLM pretraining (GPT-2 124M).

Variant	Params		Optim		Total		Step
	GiB	$\Delta$	GiB	$\Delta$	GiB	$\Delta$	ms
<b>AdamW</b>							
Reference	0.46		0.93		1.77		5.7
FlashOptim	0.23	-50%	0.36	-61%	0.74	-58%	5.9
Weight Split	0.23	-50%	1.04	+12%	1.43	-20%	5.9
Opt. Quant.	0.46		0.25	-73%	1.08	-39%	5.8
<b>Lion</b>							
Reference	0.46		0.46		1.30		4.3
FlashOptim	0.23	-50%	0.24	-48%	0.62	-53%	4.5
Weight Split	0.23	-50%	0.58	+25%	0.96	-26%	4.4
Opt. Quant.	0.46		0.12	-73%	0.96	-26%	4.4

### B.3. In-Context Learning Benchmarks

We evaluate our pretrained language models on a suite of eight in-context learning (Brown et al., 2020) benchmarks that assess diverse commonsense reasoning and language understanding capabilities:

- **HellaSwag** (Zellers et al., 2019): A sentence completion benchmark requiring physical and temporal commonsense.
- **ARC-Easy** (Clark et al., 2018): The easy subset of the AI2 Reasoning Challenge, containing grade-school science questions.
- **CommonsenseQA** (Talmor et al., 2019): Multiple-choice questions requiring commonsense knowledge from ConceptNet.
- **PIQA** (Bisk et al., 2020): Physical Interaction Question Answering, testing physical commonsense reasoning.
- **OpenBookQA** (Mihaylov et al., 2018): Elementary science questions requiring multi-step reasoning over facts.

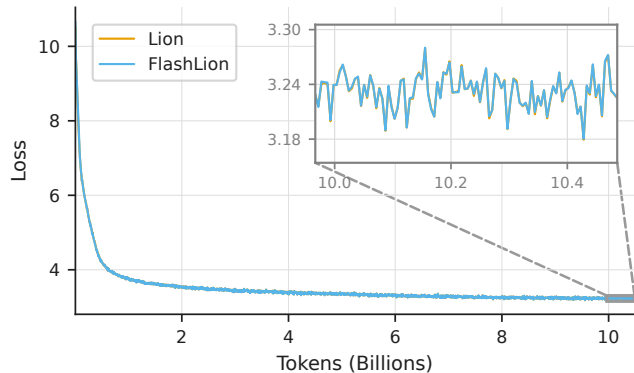


Figure 7: **Training convergence for LLM pretraining** (GPT-2 + Lion). Comparison of validation loss between reference Lion and FlashLion on FineWeb10B.

- **LAMBADA** (Paperno et al., 2016): Word prediction requiring broad discourse context understanding.
- **Winograd** (Levesque et al., 2012): Pronoun resolution problems requiring commonsense reasoning.
- **BoolQ** (Clark et al., 2019): Naturally occurring yes/no reading comprehension questions.

All benchmarks are evaluated in a zero-shot setting.

#### B.4. LLM Finetuning

We fine-tune Llama-3.1-8B (Dubey et al., 2024) on OpenMathInstruct-2 (Toshniwal et al., 2024). For evaluation, we use GSM8k (Cobbe et al., 2021), a benchmark of 1,319 grade school math word problems that require multi-step arithmetic reasoning.

**Training and Evaluation.** We use FSDP2 (Feng et al., 2022) with full parameter sharding and enabled training with activation checkpointing (Chen et al., 2016) applied to every transformer layer. We use the AdamW optimizer, with  $\beta_1 = 0.9$  and  $\beta_2 = 0.95$ . The global norm is clipped at 1.0 and a weight decay of 0.1 is used. Weight decay is applied only to weight matrices, excluding biases, embeddings, and layer normalization parameters. We train for 5000 steps with an effective batch size of approximately 5.2 million tokens per step. We apply learning rate warmup for the first 1000 steps, followed by a cosine decay to 0.

We evaluate on the GSM8k test set using temperature  $T = 0.2$  decoding. Following standard practice, we extract the final numerical answer from model generations and compare against ground truth.

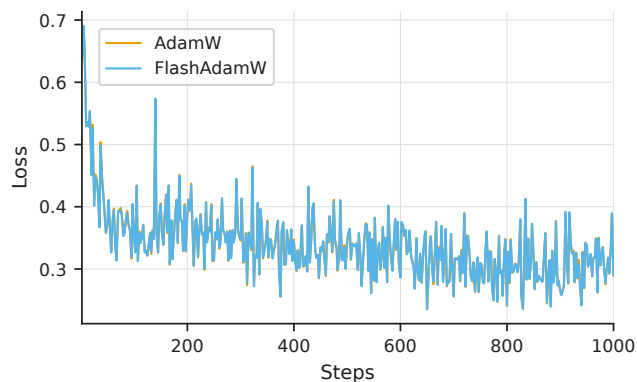


Figure 8: **Training convergence for LLM finetuning** (Llama-3.1-8B + AdamW). Comparison of training loss between reference AdamW and FlashAdamW during supervised finetuning on OpenMathInstruct-2.